Selective Disruption of Dopamine D2 Receptors in Pituitary Lactotropes Increases Body Weight and Adiposity in Female Mice

Maria Ines Perez Millan,* Guillermina Maria Luque,* Maria Cecilia Ramirez, Daniela Noain, Ana Maria Ornstein, Marcelo Rubinstein,* and Damasia Becu-Villalobos*

Laboratory of Pituitary Regulation (M.I.P.M., G.M.L., M.C.R., A.M.O., D.B.-V.), Institute of Biology and Experimental Medicine-Consejo Nacional de Investigaciones Científicas y Técnicas (CONICET), Buenos Aires 1428, Argentina; and Instituto de Investigaciones en Ingeniería Genética y Biología Molecular (D.N., M.R.), CONICET, Buenos Aires, and Departamento de Fisiología, y Biología Molecular y Celular, Facultad de Ciencias Exactas y Naturales, University of Buenos Aires, Buenos Aires 1428, Argentina

Prolactin, a pleiotropic hormone secreted by lactotropes, has reproductive and metabolic functions. Chronically elevated prolactin levels increase food intake, but in some hyperprolactinemic states such as in the global dopamine D2 receptor (D2R) knockout mouse, food intake is not increased. Here, we conduct a cell-specific genetic dissection study using conditional mutant mice that selectively lack D2Rs from pituitary lactotropes (lacDrd2KO) to evaluate the role of elevated prolactin levels without any confounding effect of central D2Rs on motor and reward mechanisms related to food intake. LacDrd2KO female mice exhibited chronic hyperprolactinemia, pituitary hyperplasia, and a preserved GH axis. In addition, lacDrd2KO female but not male mice showed increased food intake by 3 months of age, and from 5 months onward their body weights were heavier. Marked increments in fat depots, adipocyte size, serum triglycerides, and nonesterified fatty acid levels and a decrease in lipolytic enzymes in adipose tissue were seen. Furthermore, lacDrd2KO female mice had glucose intolerance but a preserved response to insulin. In the hypothalamus, *Npy* mRNA expression was increased, and *Pomc* and *Ppo* mRNA levels were unaltered (in contrast to results in global D2R knockout mice). Thus, the orexigenic effect of prolactin and its action on hypothalamic *Npy* expression were fully evidenced, leading to increased food intake and adiposity. Our results highlight the metabolic role of prolactin and illustrate the value of studying cell-specific mutant mice to disentangle the pathophysiological mechanisms otherwise masked in null allele mutants or in animals treated with pervasive pharmacological agents. **(*Endocrinology* 155: 829–839, 2014)**

Prolactin is a pleiotropic hormone secreted by lactotropes in the anterior pituitary gland and, in humans, is also produced by multiple tissues, including adipose tissue. Although the role of prolactin in reproduction and fertility has been extensively studied, less is known about its action on metabolism and body weight regulation (1). The high prolactin levels typically observed in pregnant and lactating females contribute to a hyperphagic state (2), probably sustained by leptin-resistant hypothalamic centers controlling food intake (3). During pregnancy, the normal homeostatic mechanisms regulating appetite are modified to generate a state of positive energy balance and increased food intake to supply the growing fetus with its energy requirements and increase fat storage to be used

ISSN Print 0013-7227 ISSN Online 1945-7170
Printed in U.S.A.

Received July 26, 2013. Accepted December 5, 2013.
First Published Online January 17, 2014

For News & Views see page 659

* M.I.P.M., G.M.L., M.R., and D.B.-V. contributed equally to the study.

Abbreviations: D2R, dopamine D2 receptor; DMH, dorsomedial hypothalamus; GTT, glucose tolerance test; H&E, hematoxylin and eosin; ITT, Intraperitoneal insulin tolerance test; αMSH, α-melanocyte-stimulating hormone; NEFA, nonesterified fatty acid; PCNA, proliferating cell nuclear antigen; PECAM, platelet endothelial cell adhesion molecule-1.

during lactation (4). The adaptation of metabolic processes to store energy during pregnancy in preparation for future metabolic demands is a biological allostatic hallmark in evolution.

Consistent with the hypothesis that prolactin has a significant role in the regulation of body weight, prolactin receptor–deficient mice exhibit lower body weight and reduced fat mass (5), prolactin administration stimulates food intake (6, 7), and chronically elevated prolactin levels, such as those seen during pregnancy, increase food intake, probably by inducing a state of leptin resistance (3). However, male mice bearing ectopic pituitary glands show a small increase in body weight with a decline in fat mass (8), and female mice overexpressing prolactin do not show greater body weight (9). Furthermore, we found that female mice lacking dopamine D2 receptors (*Drd2*$^{-/-}$) exhibit chronic hyperprolactinemia and pituitary lactotrope hyperplasia (10, 11) but have body weight similar to that of wild-type females in adulthood and only a minimal increase in food intake (12). However, *Drd2*$^{-/-}$mice are not an optimal model to study the effects of chronic hyperprolactinemia on energy balance, given the fundamental importance of central dopamine D2 receptors (D2Rs) in reward mechanisms related to feeding behavior (13, 14).

The available evidence suggests that lack of central D2Rs in the *Drd2*$^{-/-}$model might activate compensatory mechanisms that could ultimately limit food intake in this hyperprolactinemic transgenic model. In this regard, a critical dependence of food intake on central dopamine signaling is implied by the profound feeding deficits that result from pharmacological depletion, blockage, or genetic disruption of dopamine synthesis (15–20).

Therefore, we hypothesize that limiting *Drd2* ablation specifically in lactotropes would allow us to study the effect of high prolactin secretion on food intake and adiposity, without the confounding physiological and pathophysiological mechanisms present in global null allele *Drd2* mutants or in animals treated with pervasive pharmacological agents.

We report that conditional mutant female mice lacking D2Rs in pituitary lactotropes (lacDrd2KO) display hyperprolactinemia, increased food intake, marked body weight gain, and adipose tissue accretion compared with those in control and *Drd2*$^{-/-}$ female mice. These results highlight the hyperphagic and lipogenic effects of chronically elevated prolactin levels, which are better evidenced in the presence of functional central D2Rs.

Materials and Methods

Animals

Constitutive dopamine D2 receptor knockout mice (*Drd2*$^{-/-}$; official strain designation B6.129S2-*Drd2*^{tm1low}) used in this study were backcrossed for 10 generations to wild-type C57BL/6J mice.

lacDrd2KO mice

Mice lacking expression of D2Rs in pituitary lactotropes were generated by crossing *Drd2*$^{loxP/loxP}$ mice (13) with transgenic mice expressing *Cre* recombinase driven by the mouse prolactin promoter [Tg(Prl-cre)^{1Mrub}] (21) for 2 generations. To test the tissue specificity of *Cre* expression in Tg(Prl-cre)^{1Mrub} transgenic mice, *Cre* mRNA was analyzed by real-time PCR in different tissues. *Cre* mRNA levels were highly expressed in the pituitary and very low or almost absent in the hypothalamus, liver, kidney, ovary, and lung (Supplemental Figure 1 published on The Endocrine Society's Journals Online web site at http://end.endojournals.org). Functional Cre recombinase activity was evaluated in the pituitary, and it was present in most prolactin-producing cells of the anterior pituitary in a highly selective manner as described previously (21): immunofluorescence analysis was performed on coronal pituitary sections of double transgenic mice obtained by crossing Tg(Prl-cre)^{1Mrub} mice with the *Cre* reporter mouse line Ai14 (22) that expresses the fluorescent protein td-tomato upon Cre recombination. Analysis of double-positive cells (prolactin and td-tomato) indicated that in 96% of lactotrope Cre recombinase was active (21). lacDrd2KO mice and their *Drd2*$^{loxP/loxP}$ control littermates were congenic to C57BL/6J (n = 8).

Breeding pairs of female *Drd2*$^{loxP/loxP}$ and male *Drd2*$^{loxP/lox}$-^{P}.Tg(Prl-Cre) mice were used to generate *Drd2*$^{loxP/loxP}$ (control) and *Drd2*$^{loxP/loxP}$.Tg(Prl-Cre) (lacDrd2KO) littermates, which were included in each experiment. Mice of mixed genotypes were housed in groups of 4 or 5 in a temperature-controlled room with lights on at 7:00 AM and off at 7:00 PM and had free access to laboratory chow and tap water.

Because in male mice there was a marginal increase in prolactin levels and no differences in body or pituitary weight, fat mass depots, or food intake (Supplemental Figure 2), we used female mice in our experiments.

Body length and body weight were measured in a cohort of 12 to 14 female mice of both genotypes from 1 to 11 months of age. Every month a blood sample was collected under ketamine/xylazine anesthesia using the technique of submandibular bleeding for prolactin assay.

Mice were euthanized by decapitation at defined ages. Sera were collected for progesterone, IGF-I, prolactin, adiponectin, nonesterified fatty acids (NEFAs), triglycerides, and insulin measurements. Pituitaries, hypothalami, livers, and adipose tissues were processed for real-time PCR, histochemistry, or RIA, as detailed below.

All experimental procedures were performed according to guidelines of the institutional animal care and use committee of the Instituto de Biología y Medicina Experimental, Buenos Aires (in accordance with the Division of Animal Welfare, Office for Protection from Research Risks, National Institutes of Health, A#5072–01).

Food intake

Food intake was determined in individually caged female or male mice of both genotypes (*Drd2*$^{loxP/loxP}$ and lacDrd2KO). Mice were provided with a known amount of regular chow pellets (5% fat, 19% protein, and 5% fiber by weight; 2.4 kcal/g).

During 1 week, animals and residual food were weighed daily at the same hour (3:00 PM).

Body length

Body length was measured in live, fully anesthetized mice by the nose-anus length (from the tip of the nose to the anus), with the mice stretched supine on top of a ruler.

Estrous cycle monitoring

Estrous cycles were monitored by vaginal lavage in 5-month-old females. Cycle stage was classified as estrus (primarily cornified cells), diestrus (primarily leukocytes), or proestrus (primarily nucleated cells).

Glucose tolerance test (GTT)

GTTs were performed in conscious female lacDrd2KO and $Drd2^{loxP/loxP}$ mice at 7 months of age. In brief, after overnight fasting (8 hours), an ip injection of glucose (2 mg/g body weight) was administered. Blood glucose levels (2 μL obtained from the tail of each mouse) were examined at 0, 15, 30, 60, and 120 minutes after glucose injection with a hand-held glucose monitor (Dex-II; Bayer).

Glucose-stimulated insulin secretion

Eight-hour-fasted 7-month-old female mice were used. Blood was collected from the tail vein before (0 minutes) and 30 minutes after ip administration of glucose (3 mg/g). Serum samples were immediately obtained by centrifugation at 3000 rpm for 10 minutes and stored at −20°C. Insulin secretion levels were assessed by a sensitive mouse insulin ELISA kit (Crystal Chem).

Intraperitoneal insulin tolerance test (ITT)

Mice were fasted for 2 hours and then injected ip with human insulin (Humulin, 1 U/kg body weight; Eli Lilly). Blood glucose levels were measured with a hand-held glucose monitor (Dex-II) at 0, 15, 30, 60, 90, and 120 minutes thereafter in 2-μL samples obtained from the tail of each mouse.

Adipose tissue weight

At 5 and 11 months of age, mice were euthanized and gonadal and retroperitoneal adipose tissues, as well as livers, were carefully dissected free of surrounding tissue and weighed.

Serum lipid profile

Triglycerides and total cholesterol were measured by the Trinder colorimetric assay and NEFAs by the Duncombe colorimetric assay in 30 μL of diluted serum (1:2). The dilution was made with saline solution. Adiponectin levels were assessed by a mouse adiponectin ELISA kit (Crystal Chem).

RNA extraction and cDNA synthesis

Hypothalami, pituitaries, gonadal adipose tissues, and livers from $Tg(Prl\text{-}cre)^{1Mrub}$, wild-type, $Drd2^{loxP/loxP}$, and lacDrd2KO mice were obtained and processed for recovery of total RNA using TRIzol reagent (Invitrogen). The RNA concentration was determined on the basis of absorbance at 260 nm; its purity was evaluated by the ratio of absorbance at 260/280 nm (>1.8) and its integrity by agarose gel electrophoresis. RNAs were kept frozen at −80°C until analyzed. RNA (1 μg) was reversed transcribed in a 20-μL volume in the presence of 10 mM $MgCl_2$, 50 mM Tris · HCl (pH 8.6), 75 mM KCl, 0.5 mM deoxy-NTPs, 4 mM dithiothreitol, 0.5 μg of oligo$(dT)_{15}$ primer (Biodynamics), and 20 U of Moloney murine leukemia virus reverse transcriptase (Epicenter). The reverse transcriptase was omitted in control reactions; the absence of PCR-amplified DNA fragments in these samples indicated the isolation of RNA free of genomic DNA.

Real-time PCR for tissue *Cre*, hypothalamic proopiomelanocortin (*Pomc*), precursor of orexins (*Ppo*), neuropeptide Y (*Npy*), hepatic *Cyp2b9* and *Cyp2d9*, and liver and hepatic lipoprotein lipase (*Lpl*), hormone-sensitive lipase (*Hsl*), adipose triglyceride lipase (*Atgl*), and fatty acid synthase (*Fas*) mRNA expression levels

These measurements were performed as described previously (12). Oligonucleotides were obtained from Invitrogen. The sequences are described in Supplemental Table 1.

In brief, the reactions were performed by kinetic PCR using TAQurate Green Real-Time PCR MasterMix (9.4 μL containing 10 mM Tris · HCl, 50 mM KCl, 3 mM $MgCl_2$, 0.2 mM concentrations of deoxy-NTPs and 1.25 U of *Taq* polymerase), 100 ng of cDNA and 0.3 μM concentrations of primers in a final volume of 10 μL. The cycle profile was denaturation at 95°C for 10 minutes and amplification for 40 cycles, each cycle consisting of denaturation at 95°C for 30 seconds, annealing at 63°C for 1 minute, and extension at 72°C for 33 seconds. The accumulating DNA products were monitored by the ABI 7500 sequence detection system (Applied Biosystems), and data were stored continuously during the reaction. The results were validated on the basis of the quality of dissociation curves as described previously (12).

Histochemistry

To determine adipocyte size, histological sections (5 μm) were cut from paraffin-embedded tissue, mounted on microscope glass slides, and dried overnight in an incubator at 37°C. Sections were stained with hematoxylin and eosin (H&E). Digital images were captured using a Leica DFC320 digital camera at ×40 magnification. Morphometric analysis of gonadal adipose tissue was performed by measuring ≥50 cells from at least 3 H&E sections per mouse from each genotype (n = 4 mice) with the aid of ImageJ software (National Institutes of Health). Adipocyte area medians were calculated, and the cell size distribution for each genotype was expressed as a percentage, grouping cells at intervals of 200 μm^2.

Fluorescence immunohistochemical analysis was performed on pituitary sections from 10- and 11-month-old mice (embedded in paraffin) obtained by microtome (4 μm). Sections were incubated with primary antisera (monkey polyclonal anti-GH, 1:800; Dr. A. F. Parlow, National Hormone and Pituitary Program, Torrance, CA), diluted in PBS for 14 to 18 hours at 4 C. After 2 10-minute washes with PBS, sections were incubated with a solution containing the secondary antibody, Texas Red–conjugated goat anti-monkey IgG (1:100; Santa Cruz Biotechnology) diluted in PBS, for 1 hour at room temperature. Finally, sections were rinsed in PBS twice during 10 minutes, mounted in water, and coverslipped using fluorescence-saving medium (Vectashield; Vector Laboratories). Confocal microscopy was

performed. Sections were examined on a C1 Plan Apo 60×/1.4 oil confocal laser-scanning system (Nikon).

Immunohistochemical analysis was performed on pituitary sections from 11-month-old mice using the avidin-biotin peroxidase method as described previously (23). Rabbit polyclonal anti-proliferating cell nuclear antigen (PCNA) (1:200; Santa Cruz Biotechnology), rabbit polyclonal anti–α-melanocyte-stimulating hormone (αMSH) (1:10 000; Sigma-Aldrich), and goat polyclonal anti-platelet endothelial cell adhesion molecule-1 (PECAM) (1:200; Santa Cruz Biotechnology) were used. Appropriate secondary antibodies were chosen. Immunoreactivity was visualized using an avidin-biotin kit coupled to peroxidase (Vector Laboratories). Diaminobenzidine (Sigma-Aldrich) was used as chromogen, and tissue sections were counterstained with hematoxylin. αMSH-positive cells were expressed as a percentage of total nucleated cells in the section at a magnification of ×100. The vascular area was determined as the cumulative area of the pituitary section occupied by PECAM$^+$ vessels expressed as a percentage relative to the total area. PCNA-positive nuclei were expressed as a percentage of total nucleated cells at a magnification of ×100.

Livers were excised and snap-frozen at −80°C, embedded in OCT, and then sectioned with a cryostat (10 μm). Staining with Oil Red O (Sigma-Aldrich) was performed to visualize lipid content.

RIAs

Pituitaries were dissected and homogenized in 0.2 mL of PBS. Protein contents were measured with a Qubit fluorometer and a Quant-iT protein assay kit (Invitrogen). Aliquots of equal quantities of protein were used to assay GH and prolactin content by RIA using kits provided by the National Institute of Diabetes and Digestive and Kidney Diseases (Dr A. F. Parlow, National Hormone and Pituitary Program). Results are expressed in terms of mouse prolactin standard RP3 or mouse GH standard AFP-10783B. Intra- and interassay coefficients of variation were 7.2% and 12.8% and 8.4% and 13.2% for prolactin and GH, respectively. For IGF-I RIA, serum samples (15 μL) and IGF-I standards were subjected to the acid-ethanol cryoprecipitation method as described previously (24). IGF-I was determined using an antibody (UB2–495) provided by Drs L. Underwood and J. J. Van Wyk and distributed by the Hormone Distribution Program of the National Institute of Diabetes and Digestive and Kidney Diseases. Recombinant human IGF-I (Chiron Corp) was used as the radioligand and unlabeled ligand. The assay sensitivity was 6 pg per tube. Intra- and interassay coefficients of variation were 8.2% and 14.1%, respectively.

Progesterone was measured using an antibody provided by G. D. Niswender (Colorado State University, Fort Collins, Colorado) and labeled hormone (progesterone [1,2,6,7-^{3}H(N)]) from Dupont NEN. Assay sensitivity was 50 pg, and intra- and interassay coefficients of variation were 7.5% and 11.9%.

Statistical analysis

Results are expressed as means ± SEM. The differences between means were analyzed by the unpaired Student *t* test (in the case of only 2 groups). Two-way ANOVA with a repeated-measures design was used to analyze body weight and length, food intake, serum prolactin levels at different ages, GTTs, ITTs, and glucose-stimulated insulin secretion. Two-way ANOVA for independent measures was used to analyze liver *Cyp* mRNA expression. A post hoc Tukey test was used when necessary. Percentages were analyzed by the χ^2 test. Adipocyte size medians were compared by the median test (χ^2). A value of $P < .05$ was considered significant. Parametric or nonparametric comparisons were used as dictated by data distribution.

Results

Prolactin levels and estrous cycles in lacDrd2KO mice

Transgenic mice expressing *Cre* from a prolactin promoter, Tg(Prl-cre)^{1Mrub} (21), were used in combination with mice carrying floxed alleles in the *Drd2* gene (*Drd2*$^{loxP/loxP}$) (13) to inactivate D2Rs in pituitary lactotropes. The offspring, *Drd2*$^{loxP/loxP}$.Tg(Prl-Cre)^{1Mrub} compound mice, carried null *Drd2* alleles in lactotrope cells (lacDrd2KO), whereas *Drd2* alleles were normally expressed in other cell types as demonstrated at the molecular and functional levels (21). lacDrd2KO female mice had elevated basal prolactin levels from months 1 to 11 of age (Figure 1A), and their estrous cycles were altered, as evidenced by an increase in the percentage of diestrus occurrence (Figure 1B), and a marginal increase in serum progesterone levels at 5 months compared with those of the *Drd2*$^{loxP/loxP}$ control littermates ($P = .064$) (Figure 1C).

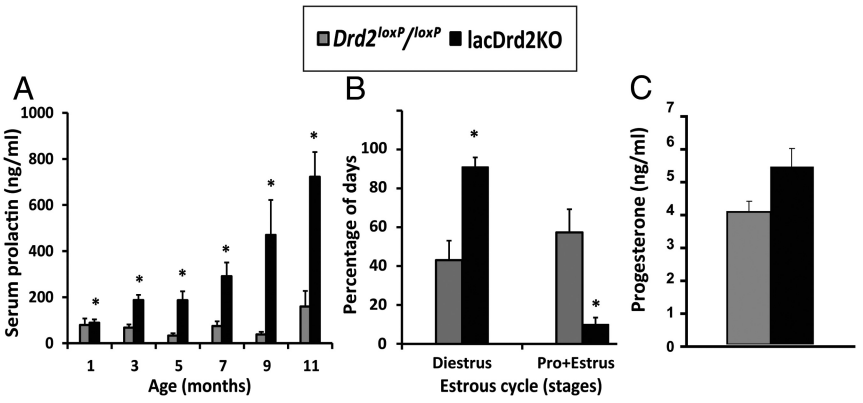

Figure 1. Serum prolactin levels are increased, and estrous cycles disrupted in female lacDrd2KO mice. A, Serum prolactin levels in female lacDrd2KO (n = 6) and *Drd2*$^{loxP/loxP}$ (n = 6) mice from 1 to 11 months of age. Two-way ANOVA indicated a significant genotype effect ($P = .0028$), and no significant interaction (genotype × age). B, Percentage of days in diestrus or proestrus + estrus observed in 5-month-old *Drd2*$^{loxP/loxP}$ (n = 5) and lacDrd2KO (n = 9) mice. χ^2 test: *, $P < .05$ vs stage of cycle-matched *Drd2*$^{loxP/loxP}$ mice. C, Progesterone levels in 11-month-old female mice ($P = .064$, n = 8 and 7, respectively). For this and the following figures all bars denote means ± SEM.

Lactotrope hyperplasia and pituitary hypertrophy in lacDrd2KO female mice

Pituitaries from 11-month-old lacDrd2KO females were heavier than pituitaries from *Drd2*$^{loxP/loxP}$ mice ($P = .0039$) (Figure 2, A and B), and the pituitary prolactin concentration was increased (Figure 2C), indicating lactotrope hyperplasia. These hyperplastic pituitaries had increased vascular area as evaluated by PECAM immunostaining ($P \leq .002$) (Figure 2D) and higher proliferation rates, as evaluated by the nuclear PCNA staining index, compared with those of controls ($P < .05$) (Figure 2E). In male mice, there were no significant differences between genotypes in pituitary weight or serum prolactin levels (Supplemental Figure 2, A and B).

LacDrd2KO female mice have a preserved GH axis

Recordings of several cohorts of female lacDrd2KO and *Drd2*$^{loxP/loxP}$ control littermates during 9 months of age revealed no differences between genotypes in body length (Figure 3A). Furthermore, no differences in femur length at 11 months were observed between genotypes (1.64 ± 0.02 and 1.69 ± 0.05 cm for *Drd2*$^{loxP/loxP}$ and lacDrd2KO mice, respectively). Accordingly, the pituitary GH concentration and percentage of somatotropes, as well as serum IGF-I levels, were similar in females of both genotypes (Figure 3, B and C, respectively). Sexual dimorphic expression of some liver genes, especially cytochrome 450 coding genes (25, 26), are regulated by GH secretory profiles. We demonstrate that mRNA levels of 2 sexually dimorphic GH-dependent liver genes, the female-predominant *Cyp2b9* and the male-predominant *Cyp2d9* gene, were similar in both genotypes, indicating preserved sexual dimorphic secretion patterns of GH (Figure 3D). Taken together, these results suggest that lacDrd2KO female mice have a normal GH axis.

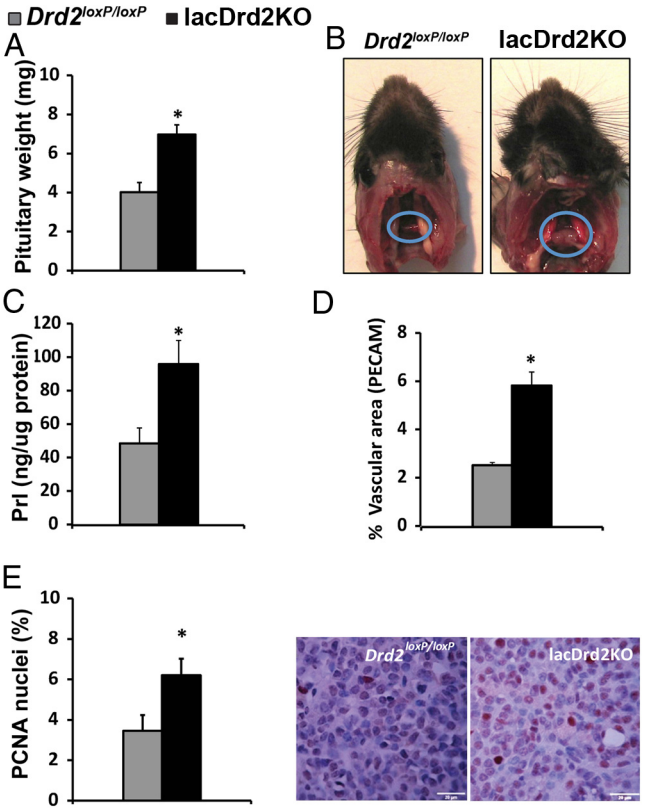

Figure 2. Lactotrope hyperplasia in aged (11-month-old) female lacDrd2KO mice. A, Pituitary weight in female *Drd2*$^{loxP/loxP}$ (n = 6) and lacDrd2KO (n = 9) mice. B, Representative image of pituitary size in a female *Drd2*$^{loxP/loxP}$ and a lacDrd2KO mouse. C, Pituitary prolactin (Prl) concentration measured by RIA in *Drd2*$^{loxP/loxP}$ (n = 6) and lacDrd2KO (n = 9) 11-month-old female mice. D, Percentage of vascular area calculated in pituitary sections immunostained using an antibody against PECAM in *Drd2*$^{loxP/loxP}$ (n = 11) and lacDrd2KO (n = 14). E, Percentage of PCNA positive nuclei in pituitaries from *Drd2*$^{loxP/loxP}$ (n = 4) and lacDrd2KO (n = 4) female mice. On the right, representative image showing increased PCNA staining in pituitaries from lacDrd2KO compared to *Drd2*$^{loxP/loxP}$ female mice. For all figures in the panel: *, $P < .05$ vs *Drd2*$^{loxP/loxP}$.

LacDrd2KO female mice have increased body weight and adiposity

Body weight curves show that starting at 5 months onward female lacDrd2KO mice were heavier than age-matched *Drd2*$^{loxP/loxP}$ controls (Figure 4A). At 5 months of age, lacDrd2KO female mice had heavier retroperitoneal fat pads and heavier livers, and by 11 months both gonadal and retroperitoneal fat pads were increased in the lacDrd2KO model (Figure 4B). In a previous work, we showed that *Drd2*$^{-/-}$ female mice had body weights in adulthood similar to those of their *Drd2*$^{+/+}$ female siblings (27). We now evaluated adipose tissue in the global knockout model and found no differences in adiposity or liver weights between *Drd2*$^{-/-}$ and *Drd2*$^{+/+}$ female mice (data not shown), in contrast to the results found in the lacDrd2KO model.

Adipocytes in lacDrd2KO mice were bigger, evidenced by an increase in the median area (1363 and 2503 μm^2 for *Drd2*$^{loxP/loxP}$ and lacDrd2KO, respectively, $P < .0001$) (Figure 4C), and adipocyte size distribution showed that adipose tissue from lacDrd2KO mice had a higher proportion of large adipocytes (larger than 2000 μm^2) (Figure 4D) than adipose tissue from *Drd2*$^{loxP/loxP}$ 11-month-old mice. Oil Red staining indicated higher lipid content in the livers of lacDrd2KO females (Figure 4E), and, in accordance, liver triglyceride content was increased ($P \leq .05$) (Figure 4F). Furthermore, lacDrd2KO female mice had increased serum triglyceride and NEFA levels compared with the *Drd2*$^{loxP/loxP}$ controls ($P \leq .05$), whereas serum cholesterol and adiponectin levels were similar in both genotypes (Figure 5, A–D).

Adiposity accretion might be the consequence of increased lipogenesis and/or decreased lipolysis. We therefore studied the expression levels of 2 lipolytic (*Hsl* and

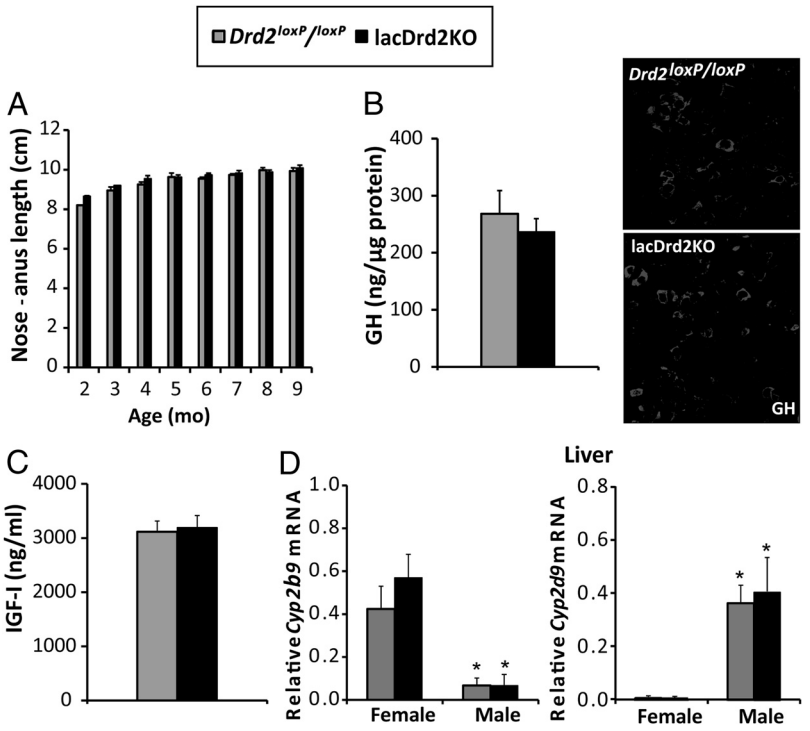

Figure 3. Female lacDrd2KO mice have a normal GH axis. A, Nose to anus length in female *Drd2*$^{loxP/loxP}$ (n = 6) and lacDrd2KO (n = 6) mice from 2 to 9 months of age. No significant differences were found. B, Pituitary GH concentration measured by RIA in female *Drd2*$^{loxP/loxP}$ (n = 6) and lacDrd2KO (n = 8) 11-month-old mice. On the right, representative immunofluorescence analysis performed on 4-μm pituitary slices of a *Drd2*$^{loxP/loxP}$ and a lacDrd2KO 11-month-old female mouse. An anti-GH primary antibody coupled with a Texas Red–conjugated secondary antibody showed similar levels of pituitary somatotropes in both genotypes. C, Serum IGF-1 levels in 11-month-old female *Drd2*$^{loxP/loxP}$ (n = 4) and lacDrd2KO (n = 4) mice. D, mRNA levels of 2 sexually dimorphic GH-dependent liver genes: left, a female-predominant gene (*Cyp2b9*); right, male predominant gene (*Cyp2d9*). No differences in levels or sexual dimorphism were evidenced between genotypes (*, $P \leq .0001$ vs females for both genotypes; n = 5 and 4 for female and 4 and 4 for male, *Drd2*$^{loxP/loxP}$ and lacDrd2KO, respectively).

Atgl) and 2 lipogenic (*Fas* and *Lpl*) enzymes. Our results showed that both lipolytic enzymes were decreased in adipose tissue but not in livers from lacDrd2KO females compared with those in *Drd2*$^{loxP/loxP}$ controls (Figure 5, E and F), whereas *Lpl* mRNA expression was decreased in both tissues from the lacDrd2KO female mouse, and no significant differences were found in *Fas* mRNA levels (Figure 5, E and F).

Male mice showed no differences in body weight, fat mass depots, or food intake among genotypes (Supplemental Figure 2, C–E).

LacDrd2KO female mice have increased food intake and hypothalamic *Npy* mRNA levels

Daily food intake was increased in 3- and 5-month-old female lacDrd2KO mice compared with that in *Drd2*$^{loxP/loxP}$ controls (Figure 6A). We therefore studied the expression of orexigenic (*Ppo* and *Npy*) and anorexigenic (αMSH and *Pomc*) factors. Hypothalamic *Npy* mRNA levels were increased in female lacDrd2KO compared with those in *Drd2*$^{loxP/loxP}$ control mice at 5 months when food intake was elevated, and the difference persisted at 11 months of age ($P < .05$) (Figure 6C), *Ppo* mRNA levels were similar in lacDrd2KO and *Drd2*$^{loxP/loxP}$ mice (Figure 6D). The percentages of melanotropes in the intermediate pituitary (cells positively stained for αMSH) were similar in lacDrd2KO and *Drd2*$^{loxP/loxP}$ mice (Figure 6B), and hypothalamic *Pomc* mRNA levels were not different between genotypes at 5 and 11 months of age (Figure 6E).

LacDrd2KO female mice exhibit impaired glucose tolerance but normal peripheral insulin sensitivity

We investigated the impact of lactotrope D2R disruption on glucose homeostasis in vivo. Fasting glucose levels in 7-month-old lacDrd2KO and *Drd2*$^{loxP/loxP}$ mice were similar (Figure 7A). However, lacDrd2KO mice showed glucose intolerance, as evidenced by higher blood glucose levels compared with those in *Drd2*$^{loxP/loxP}$ littermates, 30 and 60 minutes after the ip glucose load ($P \leq$ .05 and .02, respectively, P interaction (genotype $\times$ time) = .00002) (Figure 7A).

No differences in basal insulin levels were found, but glucose overload stimulated insulin secretion in all *Drd2*$^{loxP/loxP}$ females tested, and only in 3 of 6 lacDrd2KO littermates (Figure 7B).

To assess the effects of lactotrope D2R deficiency on insulin action in vivo, we measured the changes in plasma glucose concentrations after a single ip injection of insulin. As shown in Figure 7C, glucose disappearance curves were similar in both genotypes.

Discussion

Central nervous circuits assess and integrate peripheral metabolic, endocrine, and neuronal signals to modify energy intake and expenditure to match energy demands.

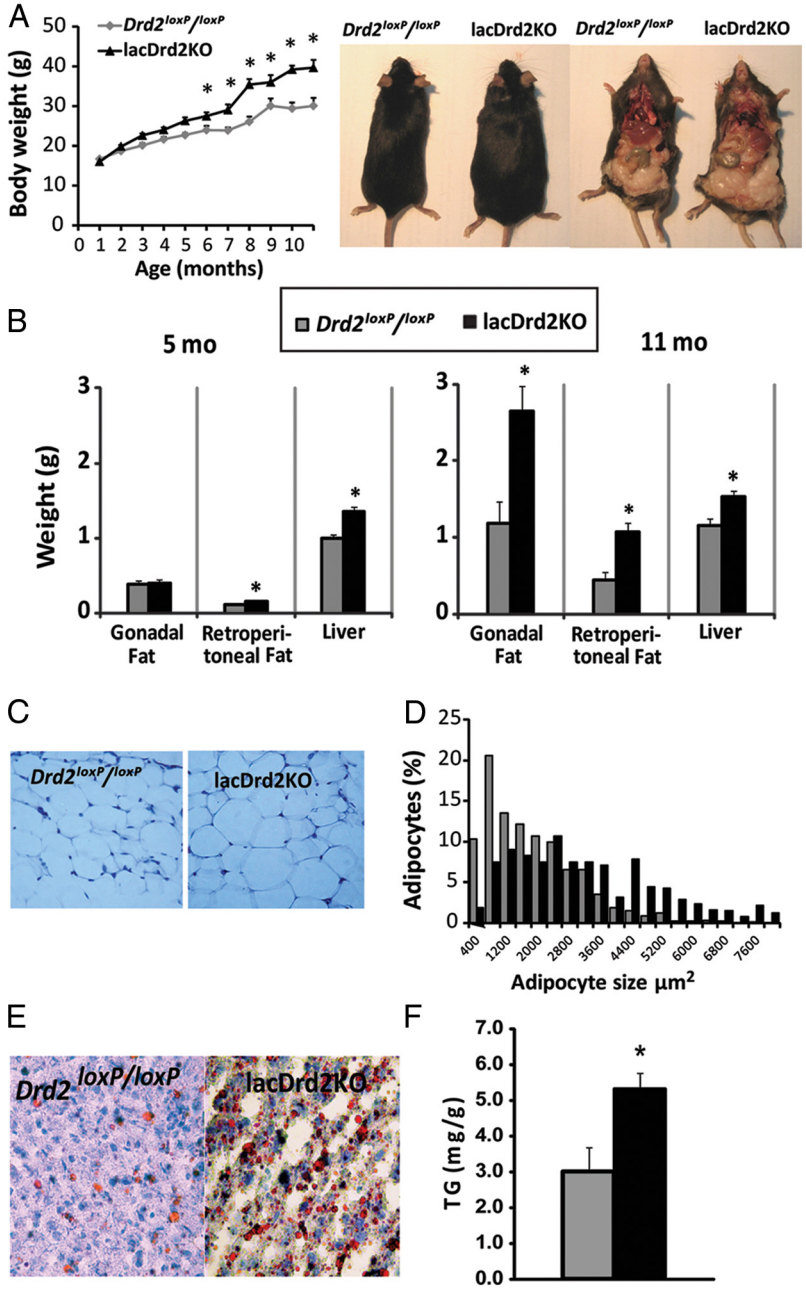

Figure 4. LacDrd2KO female mice have increased body weight and adiposity. A, Body weight curves of female lacDrd2KO (n = 12) and *Drd2*$^{loxP/loxP}$ (n = 8) mice. Two-way ANOVA showed a significant interaction (genotype × age), $P_{interaction} < .0001$; *, $P \leq .03$ vs age-matched *Drd2*$^{loxP/loxP}$ mice. On the right, representative images. B, Gonadal and retroperitoneal fat and liver weight in female *Drd2*$^{loxP/loxP}$ and lacDrd2KO 5- and 11-month-old mice (n = 5 and 5 for 5-month-old and 5 and 10 for 11-month-old mice, respectively). *, $P < .05$ vs *Drd2*$^{loxP/loxP}$ mice for each tissue, at each age. C, Representative images of H&E-stained histological samples of gonadal adipose tissue. D, gonadal adipocyte distribution according to size; 11-month-old lacDrd2KO mice had larger adipocytes compared with *Drd2*$^{loxP/loxP}$ (n = 4 and 4). E, Oil Red staining of liver sections from *Drd2*$^{loxP/loxP}$ and lacDrd2KO 11-month-old mice. F, Triglyceride (TG) content in livers from 11-month-old *Drd2*$^{loxP/loxP}$ and lacDrd2KO female mice (n = 6 and 7, respectively). *, $P = .044$ vs *Drd2*$^{loxP/loxP}$.

Many components of the neuroendocrine system act as metabolic regulators of food intake (28, 29). In particular, prolactin may be a major factor mediating the hyperphagia associated with pregnancy and lactation (2, 30). The presence of prolactin receptors in brain areas associated with the regulation of energy balance and food intake, as well as in both white and brown adipose tissue, liver, and pancreas raises the possibility that prolactin is involved in the energy balance, acting at different levels (31). In the brain, prolactin receptors have been localized in the striatum as well as in a number of hypothalamic nuclei associated with food intake and metabolism, including the arcuate nucleus, the ventromedial hypothalamus, the paraventricular hypothalamic nucleus, and the dorsomedial hypothalamus (DMH). In addition, intracerebroventricular prolactin administration increases food intake in rats (32), and the absence of prolactin receptors is accompanied by a progressive reduction in body weight in rats, females being affected to a greater degree than males (5).

Dopamine is also a physiologically relevant mediator of feeding behavior (15). It has been shown that an increase in dopamine signaling promotes feeding behavior, whereas a decrease has the opposite effect (33), and hormones implicated in regulating the homeostatic system impinge on dopamine neurons; for example, leptin and insulin directly inhibit dopamine neurons (15). Studies of dopaminergic function have implicated nigrostriatal dopaminergic pathways in feeding (34), whereas mesolimbic dopaminergic pathways (mainly the dopamine neurons in the ventral tegmental area that project to the nucleus accumbens) seem to be involved in higher-order aspects of feeding, such as motivation and reward (15, 35). Mice with selective inactivation of the tyrosine hydroxylase gene, the rate-limiting enzyme in dopamine biosynthesis, become hypophagic and die of starvation at 3 to 4 weeks (20). Furthermore, it has also been reported that deficits in striatal D2R density accelerate the onset of compulsive food seeking in rats with unrestricted access to

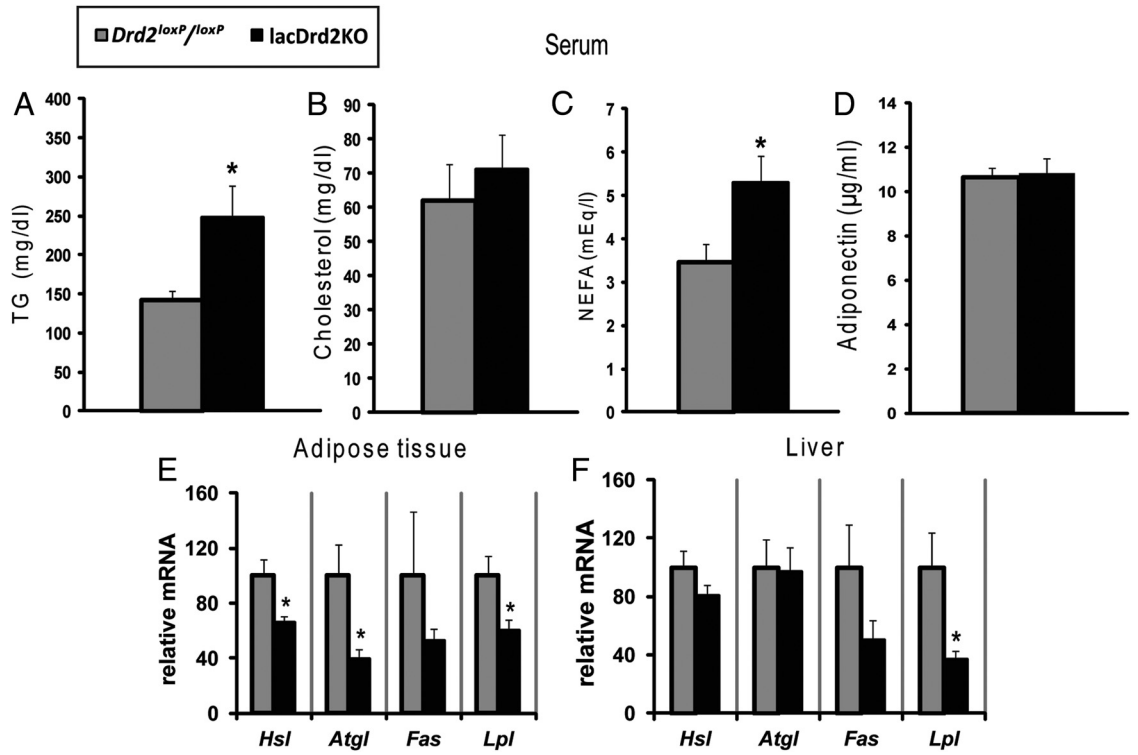

Figure 5. LacDrd2KO female mice have increased serum triglyceride and NEFA levels. Serum triglycerides (TG; n = 6 and 6) (A), cholesterol (n = 6 and 6) (B), NEFAs (n = 7 and 7) (C), and adiponectin (n = 10 and 10) (D) in ad libitum fed 11-month-old *Drd2*$^{loxP/loxP}$ and lacDrd2KO female mice, * $P \leq .05$ vs *Drd2*$^{loxP/loxP}$. E, Adipose tissue *Hsl*, *Atgl*, *Fas*, and *Lpl* mRNA expression levels in ad libitum fed 11-month-old *Drd2*$^{loxP/loxP}$ and lacDrd2KO female mice. *, $P \leq .04$ vs *Drd2*$^{loxP/loxP}$ (n = 11 and 11, respectively). F, Liver *Hsl*, *Atgl*, *Fas*, and *Lpl* mRNA expression levels in ad libitum–fed 11-month-old *Drd2*$^{loxP/loxP}$ and lacDrd2KO female mice. *, $P < .03$ *vs Drd2*$^{loxP/loxP}$ (n = 6 and 7, respectively).

palatable high-fat food (14) and might contribute to reward hypofunction in obese individuals. These data reveal the complex participation of dopamine circuits in food acquisition.

We previously noted that chronic hyperprolactinemia in female *Drd2*$^{-/-}$ mice was not accompanied by an increase in body weight or food intake (27). Therefore, we have now used a selective lactotrope D2R knockout mouse model to circumvent the overlapping effects of central D2R disruption on food intake. We demonstrate that female mice with selective lactotrope *Drd2* disruption and life-long hyperprolactinemia had increased food intake and adiposity, suggesting that the hyperphagic effect of prolactin may be more clearly evidenced when the action of dopamine on central D2Rs is preserved.

In the lacDrd2KO female mouse, we found increased prolactin secretion and a preserved GH axis. These data, together with those reported earlier in the study on male lacDrd2KO mice (21), indicate that this cell-specific mutant mouse model completely lacks D2R function in pituitary lactotropes while maintaining normally acting D2Rs in the nervous system.

In lacDrd2KO female mice, food intake was increased at 3 months of age and at 5 months body weight was higher than that for age-matched controls. This difference was maintained, and by 11 months of age the increase in body weight was approximately 24%. Progesterone, which may stimulate food intake (36), was only marginally increased in the present transgenic model. There were no differences in body length, but a marked increase in fat mass depots in lacDrd2KO mice. In contrast, we have previously reported that in adult *Drd2*$^{-/-}$ female mice there are no differences in body weight or food intake compared with those in paired wild-type adult female mice (12, 27), and we now also report that fat mass is not increased in the global knockout mouse. Because both mutant mouse strains have chronic hyperprolactinemia, the observed differences in food intake and adiposity might be related to the participation of central D2Rs, which are functional only in the lacDrd2KO model.

In this regard, we found that neural expression of neuropeptides involved in food intake and regulated by prolactin or dopamine was selectively modified in lacDrd2KO mice. Neuropeptide Y (NPY) is a potent orexigenic neuropeptide and, centrally applied, stimulates food intake (37). The major sites of its neuronal hypothalamic expression are the arcuate nucleus and the DMH. Prolactin receptors are found in NPY–containing neurons in the DMH, and both suckling (37) and prolactin (38) may activate *Npy* gene expression at this site. In the present ex-

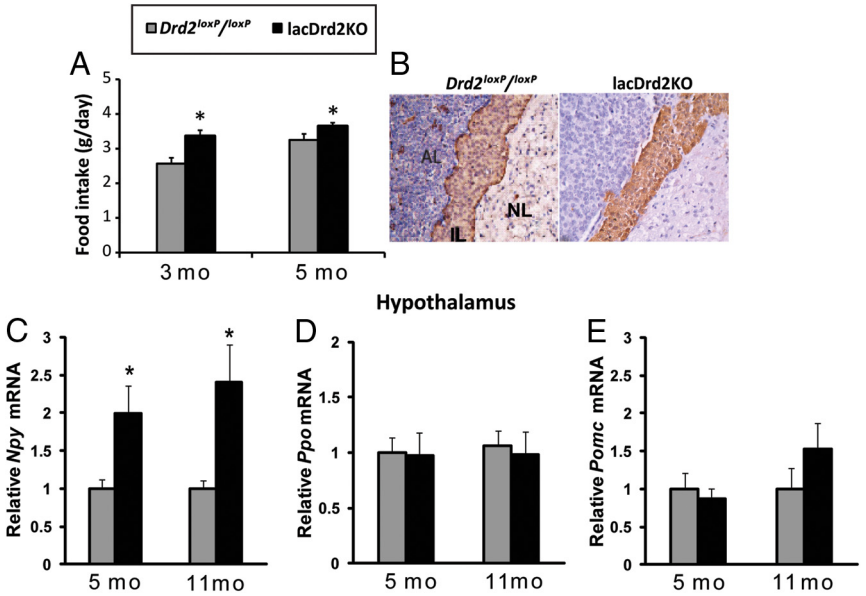

Figure 6. LacDrd2KO female mice have increased food intake and hypothalamic *Npy* mRNA levels. A, Food intake was increased in female lacDrd2KO compared with *Drd2*$^{loxP/loxP}$ mice at 3 (n = 4 and 8, respectively) and 5 (n = 6 and 7, respectively) months of age; $P = .0047$ for the effect of genotype. B, Representative immunohistochemical analysis of a section of the intermediate pituitary stained with anti-αMSH antibody. Immunostained melanotrope number was similar in 11-month-old female lacDrd2KO and *Drd2*$^{loxP/loxP}$ mice. AL, anterior pituitary lobe; IL, intermediate lobe; NL, neural lobe. C, Hypothalamic *Npy*, *Ppo*, and *Pomc* mRNA expression levels in 5- and 11-month-old *Drd2*$^{loxP/loxP}$ and lacDrd2KO female mice. *, $P = .040$ vs *Drd2*$^{loxP/loxP}$ (n=between 5 and 7).

periments, there was an increase in hypothalamic *Npy* mRNA in lacDrd2KO female mice in concordance with increased prolactin levels and food intake. We are aware of the limitations of measuring gene expression in the whole hypothalamus, which includes both the arcuate nucleus, DMH, and other nuclei; and different expression patterns might be found in each neuron subpopulation.

We also studied the hypothalamic expression of *Ppo*, the precursor of orexins A and B (39). Orexin A does not merely affect eating behavior but also has a role in sleep regulation, and a deficiency in orexin neurotransmission results in the sleep disorder narcolepsy (40). Neurons in the lateral hypothalamus showing prolactin immunoreactivity have been shown to coexpress orexins (41). We found no change in hypothalamic *Ppo* mRNA levels in lacDrd2KO mice, in contrast with the decline observed in the global *Drd2*$^{-/-}$ mice (12).

αMSH is a 13-amino acid peptide produced by posttranslational processing of POMC in the intermediate pituitary lobe and the central nervous system. It reduces food consumption and stimulates catabolism acting on the melanocortin 3 and 4 receptors. It is expressed primarily in the arcuate nucleus of the hypothalamus and expressed and secreted to the peripheral circulation by the intermediate lobe of the pituitary. Its synthesis and secretion in the intermediate pituitary is constitutively inhibited by the D2R (42). In accordance, in total *Drd2*$^{-/-}$ and not lacDrd2KO mice, the intermediate pituitary content of this anorexigenic peptide was decreased, indicating a higher release into the circulation (12).

POMC is also an anorexigenic factor, and both αMSH receptor (*Mc4r*) and *Pomc* knockout mice are obese (43, 44). Hypothalamic *Pomc* mRNA was not modified in lacDrd2KO mice.

Taken together, these results suggest that functional central D2R signaling in the lacDrd2KO mouse maintains *Pomc* and *Ppo* mRNA expression, and the central orexigenic effect of prolactin including its action on *Npy* expression is fully shown. In the global knockout mice, loss of D2R in the central nervous system mediates a decrease in *Ppo* mRNA levels and an increase in αMSH levels, and these 2 anorexigenic events may offset to some extent the effect of prolactin on food intake.

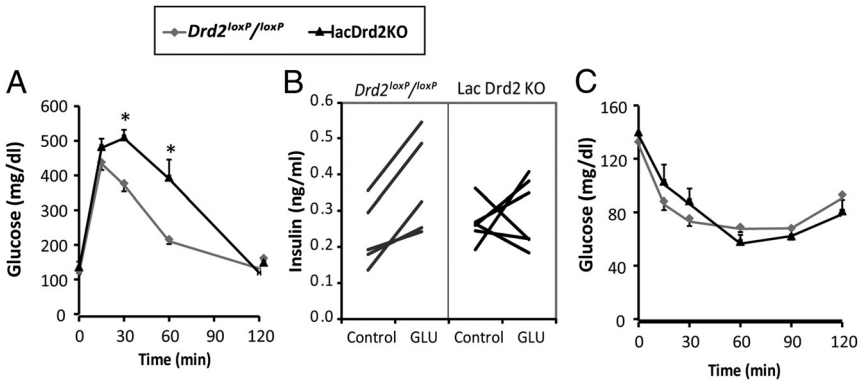

Figure 7. LacDrd2KO female mice have glucose intolerance but conserved insulin sensitivity. A, Intraperitoneal GTT (2 mg/g) in fasted *Drd2*$^{loxP/loxP}$ and lacDrd2KO female mice (n = 6 and 6, for each group). Two-way ANOVA with repeated-measures design. *, $P < .05$ vs time matched *Drd2*$^{loxP/loxP}$ mice. B, Glucose (3 mg/g ip) stimulated insulin secretion in all 7-month-old *Drd2*$^{loxP/loxP}$ female mice and in 3 of 6 lacDrd2KO mice. Differences were not significant by two-way ANOVA. C, ITT in *Drd2*$^{loxP/loxP}$ and lacDrd2KO female mice: mice were injected with 1 U/kg body weight human insulin, and blood glucose was measured at different times. No significant differences were found (n = 7 and 5, respectively).

Furthermore, our data suggest that there may be leptin resistance in the present hyperprolactinemic model, similar to that reported in pregnancy and lactation (3, 45). Increased fat mass is associated with elevated leptin levels, and leptin normally increases hypothalamic POMC and decreases NPY (45, 46) to suppress appetite. The lack of change in *Pomc* expression and the increase in *Npy* mRNA levels observed may be related to the high prolactin levels, which in pregnancy or lactation induce a state of leptin resistance to meet the metabolic demands of the dams (45).

Marked adipose accumulation was observed in the lacDrd2KO female mouse. This may be a direct consequence of increased food intake and/or increased fat absorption or altered energy expenditure. Higher food intake and adiposity have been associated with elevated serum prolactin levels. Prolactin stimulates fat deposition in female rats, pigeons, and ring doves (31), and hyperprolactinemia in men and nonpregnant women may be accompanied by weight gain (47). Furthermore, in prolactin receptor knockout mice, a reduction in body weight is associated with a reduction in total abdominal fat, and prolactin receptors have been described in adipocytes (1). Nevertheless, life-long hyperprolactinemia was present in both D2R knockout models and increased adiposity was not observed in the global knockout mouse. It is plausible that the GHRH-GH axis, which is impaired in the $Drd2^{-/-}$ but not in the lacDrd2KO model (27), may increase insulin sensitivity and prevent adiposity in the first model as opposed to the second.

Interestingly, in adipose tissue from lacDrd2KO female mice, we observed an increase in the percentage of large fat cells. Large adipocytes have been linked to type 2 diabetes risk (48). Even though there are limitations to the measurements of enzyme mRNA levels, and enzyme phosphorylation (hormone-sensitive lipase/phosphorylated hormone-sensitive lipase ratio) or enzyme activities might more accurately define the lipogenic or lipolytic status, our results show that increased storage of lipids might be the consequence of the decreased lipolytic enzyme expression found in adipose tissue from lacDrd2KO female mice, whereas the unexpected decrease in *Lpl* mRNA levels both in adipose tissue and liver in this genotype is probably associated with high prolactin levels. Prolactin inhibits lipoprotein lipase activity in human white adipose tissue and rat hepatocytes (49, 50), and furthermore, lipoprotein lipase deficiency leads to hypertriglyceridemia (51), as found in our selective knockout model.

Increased adiposity has been linked to insulin resistance (52), but even though lacDrd2KO mice had glucose intolerance and decreased insulin response to glucose overload, insulin resistance was not seen with the ITT. This result may be indicative of defective insulin secretion at the level of the pancreatic β-cell. Intolerance to glucose is observed in chronic hyperprolactinemic pituitary-grafted rats (53) and also in prolactin receptor–deficient mice (54), highlighting the complex and unresolved participation of prolactin in carbohydrate metabolism.

In conclusion, this work reveals an important role of prolactin in food intake and adiposity accretion, which may be fundamental in the metabolic adaptations to pregnancy and lactation. Furthermore, our study illustrates the value of studying cell-specific mutant mice to disentangle physiological and pathophysiological mechanisms otherwise masked in null allele mutants or in animals treated with pervasive pharmacological agents.

Acknowledgments

Address all correspondence and requests for reprints to: Damasia Becu-Villalobos, Institute of Biology and Experimental Medicine-Consejo Nacional de Investigaciones Científicas y Técnicas, Vuelta de Obligado 2490, Buenos Aires 1428, Argentina. E-mail: dbecu@dna.uba.ar.

This work was supported by the Consejo de Investigaciones Cientificas y Tecnicas (Grant PIP 640 [2009] to D.B.V.), Agencia Nacional de Promoción Científica y Técnica, Buenos Aires, Argentina (D.B.V. and M.R.), Fundación Fiorini (D.B.V.), International Research Scholar Grant of the Howard Hughes Medical (M.R.), and the Tourette Syndrome Association (M.R.).

Disclosure Summary: The authors have nothing to disclose.

References

1. **Ben-Jonathan N, LaPensee CR, LaPensee EW.** What can we learn from rodents about prolactin in humans? *Endocr Rev*. 2008;29:1–41.
2. **Woodside B.** Prolactin and the hyperphagia of lactation. *Physiol Behav*. 2007;91:375–382.
3. **Naef L, Woodside B.** Prolactin/leptin interactions in the control of food intake in rats. *Endocrinology*. 2007;148:5977–5983.
4. **Grattan DR.** The actions of prolactin in the brain during pregnancy and lactation. *Prog Brain Res*. 2001;133:153–171.
5. **Freemark M, Fleenor D, Driscoll P, Binart N, Kelly P.** Body weight and fat deposition in prolactin receptor-deficient mice. *Endocrinology*. 2001;142:532–537.
6. **Byatt JC, Staten NR, Salsgiver WJ, Kostelc JG, Collier RJ.** Stimulation of food intake and weight gain in mature female rats by bovine prolactin and bovine growth hormone. *Am J Physiol*. 1993;264:E986–E992.
7. **Gerardo-Gettens T, Moore BJ, Stern JS, Horwitz BA.** Prolactin stimulates food intake in a dose-dependent manner. *Am J Physiol*. 1989;256:R276–R280.
8. **Matsuda M, Mori T, Sassa S, Sakamoto S, Park MK, Kawashima S.** Chronic effect of hyperprolactinemia on blood glucose and lipid levels in mice. *Life Sci*. 1996;58:1171–1177.
9. **Ling C, Hellgren G, Gebre-Medhin M, et al.** Prolactin (PRL) receptor gene expression in mouse adipose tissue: increases during lactation and in PRL-transgenic mice. *Endocrinology*. 2000;141:3564–3572.
10. **Kelly MA, Rubinstein M, Asa SL, et al.** Pituitary lactotroph hyper-

plasia and chronic hyperprolactinemia in dopamine D2 receptor-deficient mice. *Neuron*. 1997;19:103–113.
11. **Cristina C, Díaz-Torga G, Baldi A, et al.** Increased pituitary vascular endothelial growth factor-A in dopaminergic D2 receptor knockout female mice. *Endocrinology*. 2005;146:2952–2962.
12. **Garcia-Tornadú I, Díaz-Torga G, Risso Gs, et al.** Hypothalamic orexin, OX1, αMSH, NPY and MCRs expression in dopaminergic D2R knockout mice. *Neuropeptides*. 2009;43:267–274.
13. **Bello EP, Mateo Y, Gelman DM, et al.** Cocaine supersensitivity and enhanced motivation for reward in mice lacking dopamine D2 autoreceptors. *Nat Neurosci*. 2011;14:1033–1038.
14. **Johnson PM, Kenny PJ.** Dopamine D2 receptors in addiction-like reward dysfunction and compulsive eating in obese rats. *Nat Neurosci*. 2010;13:635–641.
15. **Palmiter RD.** Is dopamine a physiologically relevant mediator of feeding behavior? *Trends Neurosci*. 2007;30:375–381.
16. **Phillips AG, Nikaido RS.** Disruption of brain stimulation-induced feeding by dopamine receptor blockade. *Nature*. 1975;258:750–751.
17. **Zigmond MJ, Stricker EM.** Deficits in feeding behavior after intraventricular injection of 6-hydroxydopamine in rats. *Science*. 1972; 177:1211–1214.
18. **Wise RA, Colle LM.** Pimozide attenuates free feeding: best scores analysis reveals a motivational deficit. *Psychopharmacology (Berl)*. 1984;84:446–451.
19. **Ungerstedt U.** Adipsia and aphagia after 6-hydroxydopamine induced degeneration of the nigro-striatal dopamine system. *Acta Physiol Scand Suppl*. 1971;367:95–122.
20. **Zhou QY, Palmiter RD.** Dopamine-deficient mice are severely hypoactive, adipsic, and aphagic. *Cell*. 1995;83:1197–1209.
21. **Noaín D, Pérez-Millán MI, Bello EP, et al.** Central dopamine D2 receptors regulate growth-hormone-dependent body growth and pheromone signaling to conspecific males. *J Neurosci*. 2013;33:5834–5842.
22. **Madisen L, Zwingman TA, Sunkin SM, et al.** A robust and high-throughput Cre reporting and characterization system for the whole mouse brain. *Nat Neurosci*. 2010;13:133–140.
23. **Luque GM, Pérez-Millán MI, Ornstein AM, Cristina C, Becu-Villalobos D.** Inhibitory effects of antivascular endothelial growth factor strategies in experimental dopamine-resistant prolactinomas. *J Pharmacol Exp Ther*. 2011;337:766–774.
24. **Lacau-Mengido IM, Mejía M, Diaz-Torga G, et al.** Endocrine studies in ivermectin-treated heifers from birth to puberty. *J Anim Sci*. 2000;78:1–8.
25. **Waxman DJ, Holloway MG.** Sex differences in the expression of hepatic drug metabolizing enzymes. *Mol Pharmacol*. 2009;76:215–228.
26. **Ramirez MC, Luque GM, Ornstein AM, Becu-Villalobos D.** Differential neonatal testosterone imprinting of GH-dependent liver proteins and genes in female mice. *J Endocrinol*. 2010;207:301–308.
27. **Díaz-Torga G, Feierstein C, Libertun C, et al.** Disruption of the D2 dopamine receptor alters GH and IGF-I secretion and causes dwarfism in male mice. *Endocrinology*. 2002;143:1270–1279.
28. **Cone RD.** The central melanocortin system and energy homeostasis. *Trends Endocrinol Metab*. 1999;10:211–216.
29. **Cone RD, Cowley MA, Butler AA, Fan W, Marks DL, Low MJ.** The arcuate nucleus as a conduit for diverse signals relevant to energy homeostasis. *Int J Obes Relat Metab Disord*. 2001;25(suppl 5):S63–S67.
30. **García MC, López M, Gualillo O, Seoane LM, Diéguez C, Señarís RM.** Hypothalamic levels of NPY, MCH, and prepro-orexin mRNA during pregnancy and lactation in the rat: role of prolactin. *FASEB J*. 2003;17:1392–1400.
31. **Ben-Jonathan N, Hugo ER, Brandebourg TD, LaPensee CR.** Focus on prolactin as a metabolic hormone. *Trends Endocrinol Metab*. 2006;17:110–116.
32. **Sauvé D, Woodside B.** The effect of central administration of prolactin on food intake in virgin female rats is dose-dependent, occurs in the absence of ovarian hormones and the latency to onset varies with feeding regimen. *Brain Res*. 1996;729:75–81.
33. **Narayanan NS, Guarnieri DJ, DiLeone RJ.** Metabolic hormones, dopamine circuits, and feeding. *Front Neuroendocrinol*. 2010;31: 104–112.
34. **Hnasko TS, Perez FA, Scouras AD, et al.** Cre recombinase-mediated restoration of nigrostriatal dopamine in dopamine-deficient mice reverses hypophagia and bradykinesia. *Proc Natl Acad Sci USA*. 2006;103:8858–8863.
35. **Schwartz MW, Woods SC, Porte D Jr, Seeley RJ, Baskin DG.** Central nervous system control of food intake. *Nature*. 2000;404:661–671.
36. **Hirschberg AL.** Sex hormones, appetite and eating behaviour in women. *Maturitas*. 2012;71:248–256.
37. **Chen P, Smith MS.** Regulation of hypothalamic neuropeptide Y messenger ribonucleic acid expression during lactation: role of prolactin. *Endocrinology*. 2004;145:823–829.
38. **Li C, Chen P, Smith MS.** Neuropeptide Y and tuberoinfundibular dopamine activities are altered during lactation: role of prolactin. *Endocrinology*. 1999;140:118–123.
39. **Sakurai T, Amemiya A, Ishii M, et al.** Orexins and orexin receptors: a family of hypothalamic neuropeptides and G protein-coupled receptors that regulate feeding behavior. *Cell*. 1998;92:573–585.
40. **Taheri S, Zeitzer JM, Mignot E.** The role of hypocretins (orexins) in sleep regulation and narcolepsy. *Annu Rev Neurosci*. 2002;25:283–313.
41. **Risold PY, Griffond B, Kilduff TS, Sutcliffe JG, Fellmann D.** Preprohypocretin (orexin) and prolactin-like immunoreactivity are coexpressed by neurons of the rat lateral hypothalamic area. *Neurosci Lett*. 1999;259:153–156.
42. **Cote TE, Felder R, Kebabian JW, et al.** D-2 dopamine receptor-mediated inhibition of pro-opiomelanocortin synthesis in rat intermediate lobe. Abolition by pertussis toxin or activators of adenylate cyclase. *J Biol Chem*. 1986;261:4555–4561.
43. **Yaswen L, Diehl N, Brennan MB, Hochgeschwender U.** Obesity in the mouse model of pro-opiomelanocortin deficiency responds to peripheral melanocortin. *Nat Med*. 1999;5:1066–1070.
44. **Chen AS, Metzger JM, Trumbauer ME, et al.** Role of the melanocortin-4 receptor in metabolic rate and food intake in mice. *Transgenic Res*. 2000;9:145–154.
45. **Augustine RA, Ladyman SR, Grattan DR.** From feeding one to feeding many: hormone-induced changes in bodyweight homeostasis during pregnancy. *J Physiol*. 2008;586:387–397.
46. **Schwartz MW, Seeley RJ, Woods SC, et al.** Leptin increases hypothalamic pro-opiomelanocortin mRNA expression in the rostral arcuate nucleus. *Diabetes*. 1997;46:2119–2123.
47. **Doknic M, Pekic S, Zarkovic M, et al.** Dopaminergic tone and obesity: an insight from prolactinomas treated with bromocriptine. *Eur J Endocrinol*. 2002;147:77–84.
48. **Laurencikiene J, Skurk T, Kulyté A, et al.** Regulation of lipolysis in small and large fat cells of the same subject. *J Clin Endocrinol Metab*. 2011;96:E2045–E2049.
49. **Ling C, Svensson L, Odén B, et al.** Identification of functional prolactin (PRL) receptor gene expression: PRL inhibits lipoprotein lipase activity in human white adipose tissue. *J Clin Endocrinol Metab*. 2003;88:1804–1808.
50. **Julve J, Robert MQ, Llobera M, Peinado-Onsurbe J.** Hormonal regulation of lipoprotein lipase activity from 5-day-old rat hepatocytes. *Mol Cell Endocrinol*. 1996;116:97–104.
51. **Weinstock PH, Bisgaier CL, Aalto-Setälä K, et al.** Severe hypertriglyceridemia, reduced high density lipoprotein, and neonatal death in lipoprotein lipase knockout mice. Mild hypertriglyceridemia with impaired very low density lipoprotein clearance in heterozygotes. *J Clin Invest*. 1995;96:2555–2568.
52. **Kahn SE, Hull RL, Utzschneider KM.** Mechanisms linking obesity to insulin resistance and type 2 diabetes. *Nature*. 2006;444:840–846.
53. **Reis FM, Reis AM, Coimbra CC.** Effects of hyperprolactinaemia on glucose tolerance and insulin release in male and female rats. *J Endocrinol*. 1997;153:423–428.
54. **Freemark M, Avril I, Fleenor D, et al.** Targeted deletion of the PRL receptor: effects on islet development, insulin production, and glucose tolerance. *Endocrinology*. 2002;143:1378–1385.